JOURNAL DE PHYSIQUE

Colloque C2, supplément au n°3, Tome 44, mars 1983 *page* C2-183

OPTICAL TURBULENCE : CHAOS IN OPTICAL BISTABILITY

K. Ikeda

Department of Physics, Kyoto University, Kyoto 606, Japan

Résumé - La lumière transmise hors d'une cavité optique bistable peut, lorsque l'on augmente l'intensité de la lumière-laser incidente, faire apparaitre une variété d'un phénomène de bifurcation, à savoir : le passage d'un état stationnaire, suivi d'une suite d'états périodiques puis chaotiques, à un état chaotique final "complètement développé". Revue d'un point de vue théorique des travaux récents sur ces phénomènes.

Abstract - The transmitted light from a bistable optical cavity can exhibit a variety of bifurcation phenomena, passing from a stationary state, through successive periodic and chaotic states to a final fully developed chaotic state, as the intensity of incident laser light is increased. Recent studies on these phenomena are reviewed from a theoretical point of view.

Turbulence was for many years one of the hard problems in physics. The first decisive attack was made by Ruelle and Takens /1/ who rejected Landau-Hopf's interpretation /2/ and suggested that the turbulent state can appear not only in fluids, but also in non-equilibrium dissipative systems with a few degrees of freedom. Being different from thermal noise, the turbulent state now in question has its origin in the nonlinearity of the system and the resulting instability of orbit in the phase space. A state which is erratic in time is called chaotic state; the scheme of transition (bifurcation) to this state has been a subject of active investigations in recent years /3/, especially in fluid systems /4/.

In addition to fluid systems, nonlinear optical systems also provide typical examples of non-equilibrium physical systems. It is expected that these systems will provide good subjects for the study of turbulence. Among the various systems in nonlinear optics, the optical bistable system /5/ is supposed to be one of the typical examples exhibiting chaotic behavior. The occurrence of chaos in this system was first predicted theoretically by the author's group /6/, and further investigations have been made by us /7-9/ and also by several other authors /10-14/. The experimental evidence of chaotic behavior was first presented by the Arizona University group in a hybrid bistable device /15/. Quite recently a transition to chaos has been observed in an all optic device by a group at Kyoto University /16/.

In this article we review the present state of theoretical investigations on chaos of an optical bistable system which has been developed by the present author's group.

I- DELAY INDUCED INSTABILITY : A SIMPLE DESCRIPTION

For simplicity, we consider hereafter a ring cavity resonator containing a nonlinear dielectric medium of lenghth ℓ, as shown in Fig.1. Let us assume that the responce time γ^{-1} of the nonlinear medium to the electric field is so short that it can follow the temporal change of the electric field adiabatically. The phase shift of

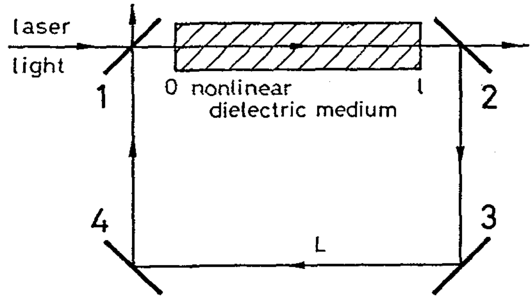

Fig.1 - Ring resonator model.

the electric field is then given by $n(|\hat{E}|)k\ell$, where $n(|\hat{E}|)$ is the nonlinear refractive index and k the wave number of light. Thus the electric field at the right end of the medium is related to that at the entrance on the left by

$$\hat{E}(t,\ell) = \exp[-\frac{\alpha\ell}{2} + in(|E(t-\frac{\ell}{c},0)|)k\ell]\hat{E}(t-\frac{\ell}{c},0), \tag{1.1}$$

taking into account the time delay due to the propagation. Here α is the absorption coefficient of the medium, and c the velocity of light in the medium. Another relation connecting the field at the entrance of the medium with that at the exit is the boundary condition

$$E(t,0) = (1 - R)^{1/2}E_I + RE(t - (L - \ell)/c, \ell) , \tag{1.2}$$

where $\hat{E}_I$ is the electric field of the incident light, L the cavity length and R the reflectivity of mirrors 1 and 2 (Mirrors 3 and 4 are assumed to have 100% reflectivity). Combining Eqs.(1.1) and (1.2) and expanding $n(|\hat{E}|)$ up to the order of $|\hat{E}|^2$, we obtain the following two-dimensional mapping rule describing the dynamics of the cavity field /6/:

$$\begin{aligned} E(t) &= A + BE(t - t_R)\exp i[|E(t - T_R)|^2 - \phi_0] \\ &\equiv U(E(t - t_R)), \end{aligned} \tag{1.3}$$

where the electric field E has been scaled into a dimensionless form. Parameter $A \equiv \{(1-R)k|n_2|(1-e^{-\alpha\ell})/\alpha\}^{1/2}E_I$ (n_2:the quadratic coefficient of the nonlinear refractive index) is proportional to the incident field amplitude and $B \equiv Re^{-\alpha\ell}(< 1)$ is a parameter describing the dissipation in the cavity. Note that the time delay $t_R \equiv L/c$ originates from the propagation of the light in the cavity.

The mapping rule $E_{n+1} = U(E_n)$ can be reduced to a more simplified form: One can prove that after a large number of operations of U, E_n falls into a confined region

$$AB(1 - 2B)/(1 - B) < |E_n - A| < AB/(1 - B) , \tag{1.4}$$

for $B < 1/2$. Having this in mind, we can easily prove that the intensity $I_n \equiv |E_n|^2$ obeys the following one-dimensional mapping rule /6/:

$$I_n = A^2[1 + 2B\cos(I_n - \phi_0)] \equiv f(A^2;I_n), \tag{1.5}$$

in the limit of $B << 1$ with A^2B kept fixed. The stationary solution of eq(1.5), which is denoted by I_s, is a multivalued function of the input intensity A^2 (optical multistability):

$$I_s/(1 + 2B\cos(I_s - \phi_0)) = A^2 \tag{1.6}$$

These I_s are not always stable. To show this we construct the iterated solution $I_2 = f(I_1), I_3 = f(I_2), \cdots I_{n+1} = f(I_n) \cdots$ by the graphical method illustrated in Fig. 2.

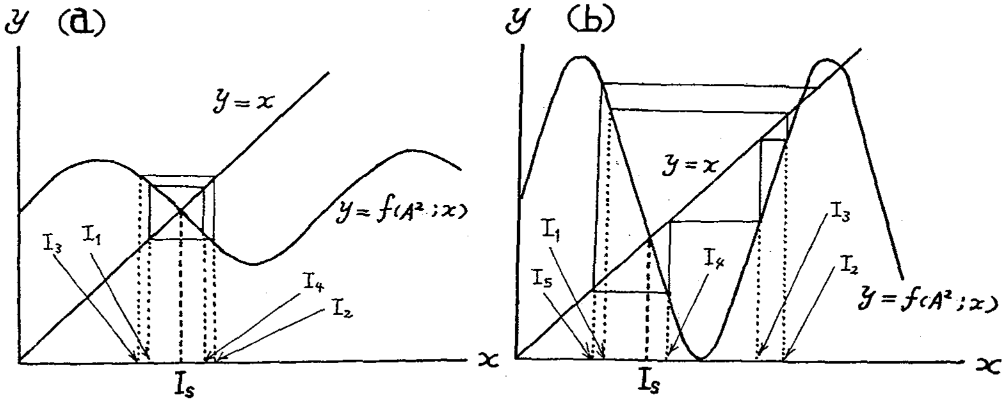

Fig.2 - Graphical solution of $I_{n+1} = f(A^2;I_n)$

If the parameter $C \equiv 2A^2B$ is small enough the stationary solution I_s is stable since, as is shown in Fig.2(a), the sequence $\{I_n\}$ approaches to I_s asymptotically as $n \to \infty$. For sufficiently large C, however, all the stationary solutions become unstable. As is shown in Fig.2(b), the sequence $\{I_n\}$ wanders in a quite erratic manner over the unstable stationary solutions, in other words, the time dependence of the intensity is chaotic. We call this phenomenon a delay induced instability becuase its origin is essentially in the time delay due to the propagation effect.

The chaotic state is characterized by the fact that a small difference in the initial condition is amplified by a large number of operations of f (orbital instability). Hence in the chaotic state the geometrical average of the single step amplification rate $|dI_{n+1}/dI_n| = |f'(I_n)|$ is larger than unity, or in other words, the Liapunov exponent

$$\lambda \equiv \lim_{N} \frac{1}{N} \sum_{k=1}^{N} \log|f'(I_n)| \tag{1.7}$$

is positive. In case of Eq.(1.5) the Liapunov exponent is given by

$$\lambda = \log A^2B + \langle \log|2\sin(I_n - \phi_0)|\rangle , \tag{1.8}$$

where the braket denotes an average over a large number of iteration steps. Therefore, the condition for chaos is roughly given by $A^2B > O(1)$ because the second part in the right hand side of Eq.(1.8) is a quantity of O(1). A detailed analysis shows that the condition for chaos in our ring resonator model is given by /6/:

$$A^2B > 1 \tag{1.9}$$

Quite recently, the transition to chaos has been observed in an all optic ring resonator /16/. The onset condition of chaos observed in this experiment is consistent with the inequality (1.9).

Chaotic behavior due to delay induced instability was predicted also for folded Fabry-Perot resonators /10/ and for distributed-feedback resonators /11/. An interesting assertion has been recently made by Silberberg and Bar Joseph /12/ that the feedback mechanism by mirrors is not necessary to induce chaos; two light beams interacting via a third-order susceptibility exhibits a transition to chaos as the input intensity is increased.

II - SUCCESSIVE BIFURCATIONS

The description based on Eq.(1.3) is simple and allows an analytical treatment to some extent. In reality, however, the description based on the assumption of "the adiabatic following" is valid only in a limited initial range of time, because in chaos temporal fluctuation grows exponentially /6/, and for longer times we have to take into account the finiteness of the relaxation time. This can easily be done by replacing the nonlinear phase shift $|E(t-t_R)|^2$ in Eq.(1.3) by

$$\phi(t) = \gamma\int_{-\infty}^{t} e^{-\gamma(t-s)}|E(s - t_R)|^2 ds .$$

Correspondingly, eq.(1.3) should be rewritten as a set of coupled delay-differential equations/6/:

$$E(t) = A + BE(t - t_R)\exp i(\phi(t) - \phi_0) , \qquad (2.1a)$$

$$\gamma^{-1}\dot{\phi}(t) = - \phi(t) + |E(t - t_R)|^2 . \qquad (2.1b)$$

In the limit of $B \ll 1$ with A^2B kept fixed, Eq.(2.1) reduce to the one variable delay-differential equation corresponding to the one dimensional map (1.5):

$$\gamma^{-1}\dot{\phi}(t) = - \phi (t) + f(\pi\mu;\phi(t - t_R)) , \qquad (2.2)$$

where $\mu \equiv A^2/\pi$. We discuss below how the solution of Eq.(2.2) exhibits transitions (bifurcations) to the chaotic state as the input parameter μ is increased slowly in time.

Successive period-doubling bifurcations - When μ is increased beyond a certain value μ_A, the stationary state (1.6) becomes unstable, and a square wave of period $T_0(\simeq 2t_R)$ appears (Hopf bifurcation). As μ is increased further, the period of the square wave T doubles successively $T_0 \to 2T_0 \to 2^2T_0 \to \cdots \to 2^nT_0$ as is shown in Fig.3.

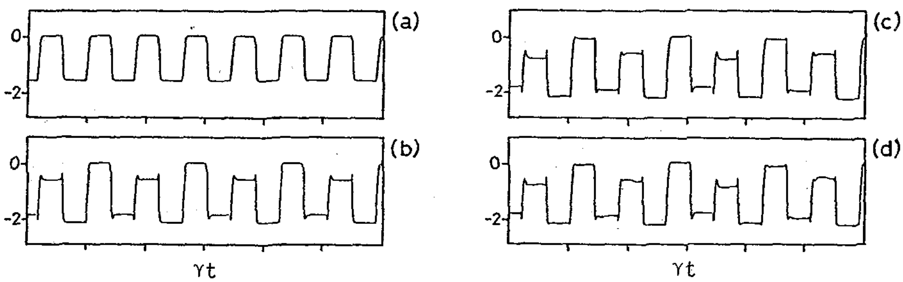

Fig.3 - Change of wave forms in successive period doubling bifurcations for $t_R\gamma = 40$, $B = 0.5$ and $\phi_0 = -\pi/2$; (a) period-2cycle ($\mu = .50$), (b) period-4 cycle ($\mu = .67$), (c) period-8 cycle ($\mu = .69$) and (d) chaos ($\mu = .70$)

At a certain value μ_F, n becomes infinite, i.e. $T \to \infty$, so that the wave form becomes chaotic. This phenomenon is an example of period doubling bifurcations which follow Feigenbaum's universal rule /3/.

Successive higher-harmonic bifurcations - Coarsely seen, the wave form of the chaotic oscillation is still square-wave-like with fundamental period T_0 (Fig.4(a)), if μ is not far beyond μ_F. When μ is further increased, there appears a chaotic state

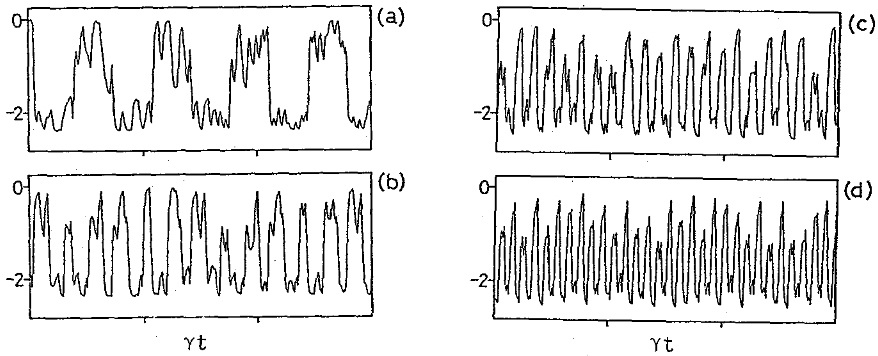

Fig.4 - Successive higher-harmonic bifurcations. The parameter values are the same as in Fig.3; (a) fundamental ($\mu = .770$), (b) 3rd harmonic ($\mu = .778$), (c) 5th harmonic ($\mu = .780$), and (d) 7th harmonic ($\mu = .822$).

whose wave form is much more complicated with a short characteristic time (Fig.6(a)). We call such a state developed chaos. On the way from the square wave chaos to the developed chaos, there appears a new bifurcation sequence: With the increase of the period of the coarsely square wave changes discontinuously in the sequence $T_0 \to T_0/3 \to T_0/5 \to \cdots \to T_0/n_{max}$ (n_{max}: an odd integer) as is illustrated in Fig.4(a)-(d) /7/. Correspondingly, the position of the highest peak in the power spectrum jumps abruptly in the order $\omega_0 (\equiv 2\pi/T_0 \approx \pi/t_R) \to 3\omega_0 \to 5\omega_0 \to \cdots \to n_{max}\omega_0$. The solution of period T_0/n (n : odd integer) is thus regarded as a higher harmonic solution of the fundamental solution with period T_0. These phenomena are called successive higher-harmonic bifurcations. These bifurcations are quite novel because they are successive first-order transitions accompanied by hysteresis.

In Fig.5 we show the domain of μ in which the higher harmonic solutions exist and the hysteresis between them. The ordinate Ω denotes the mean frequency of the corresponding higher harmonic solution, so that $\Omega = n$ denotes a pure n-th harmonic. An

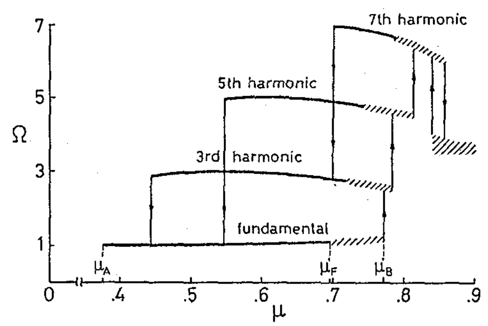

Fig.5 - Domain of harmonic solutions and hysteresis between them. The parameter values are the same as in Fig.3. The solid line and shaded parts indicates periodic and chaotic solutions, repectively.

interesting point is that the branch of every higher harmonic solution consists of purely periodic and chaotic parts. The successive higher harmonic bifurcation terminates at $n = n_{max}$, and with further increase of μ a final transition to the developed chaos takes place. The integer n_{max} increases in proportion to $t_R\gamma$; in the case of Fig.5 ($t_R\gamma = 40$) n_{max} is 7. The occurrence of the successive higher-harmonic bifurcations can be explained using the fact that in the limit of $t_R\gamma >> 1$ the delay-differential equation (2.2) formally reduces to the difference equation

$$\phi(t) = f(\pi\mu;\phi(t - t_R)) \quad ,$$

which exhibits the period doubling bifurcations /7/. The successive higher-harmonic bifurcations are generic phenomena in any equations of the form (2.2) /7/.

In experiment, Hopf et al observed the detailed series of period doubling bifurcations, which agrees well with the theoretical results /15/. They also observed that the period of the square wave is locked to the higher harmonics of their fundamental. This phenomenon can be regarded as evidence of the successive higher-harmonic bifurcation. The period doubling phenomena were also observed in a recent experiment for an all optic ring resonator /16/.

III - FULLY DEVELOPED CHAOS

The power spectrum of the developed chaos still have sharp peaks at the fundamental and higher-harmonic positions $\omega = n\omega_0$ (n:odd integer). A remarkable fact is that the peak intensities at $\omega = n\omega_0$ are all about the same for $n \leq n_{max}$ (Fig.6(a)), which implies that the motion in the phase space is wandering over the higher-harmonic attractors as well as over the fundamental one, all of which have already been destroyed. The period for which any higher-harmonic attractor is visited seems to be

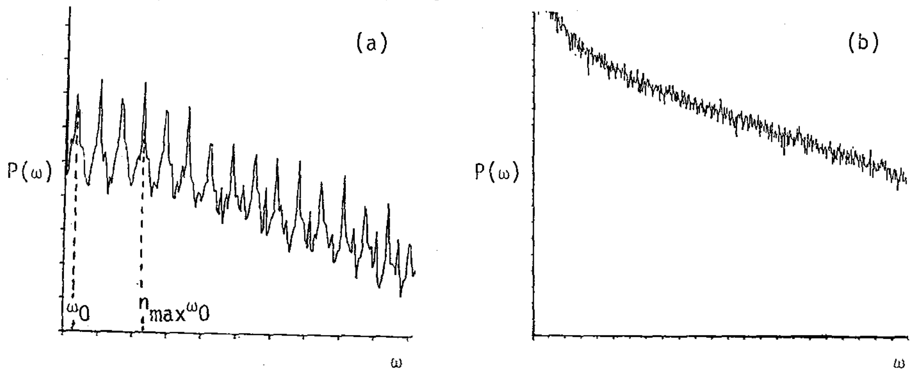

Fig.6 - Power spectrum of $\phi(t)$; (a) developed chaos ($\mu = .88$), (b) fully developed chaos ($\mu = 5.6$).

about the same. In the limit of large μ, however, the peak structure disappears and the power spectrum becomes a smooth function of ω(Fig.6(b)). Correspondingly, the time dependence of $\phi(t)$ becomes quite random and homogeneous as in Fig.7.

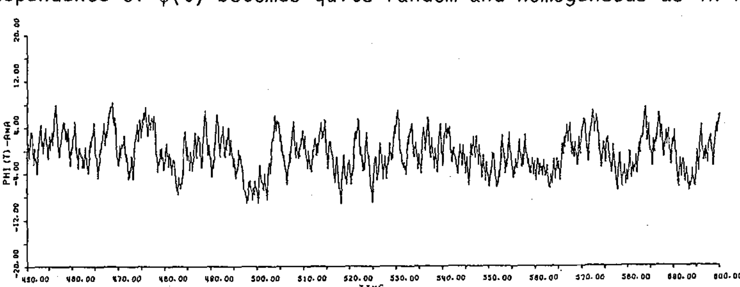

Fig. 7 - Time variation of $\phi(t)$ in the fully developed chaos($\mu = 5.6$).

It reminds us of a bounded Brownian motion. We call such a stage "fully developed chaos".

In this stage we may expect that the motion of $\phi(t)$ is so random that it can be described by a simple stochastic process. To show this let us introduce the normalized correlation function.

$$R^{(2n)}(t) = \langle\Delta\phi^n(t)\ \Delta\phi^n(0)\rangle\ /\ \langle(\Delta\phi)^2\rangle^n$$

, where $\Delta\phi \equiv \phi(t) - \langle\phi\rangle$ and $\langle\ \rangle$ denotes a long time average. Some examples of the correlation functions obtained from a numerical simulation are shown in Fig.8 by solid curves. It is well known that in a Gaussian stochastic process higher order

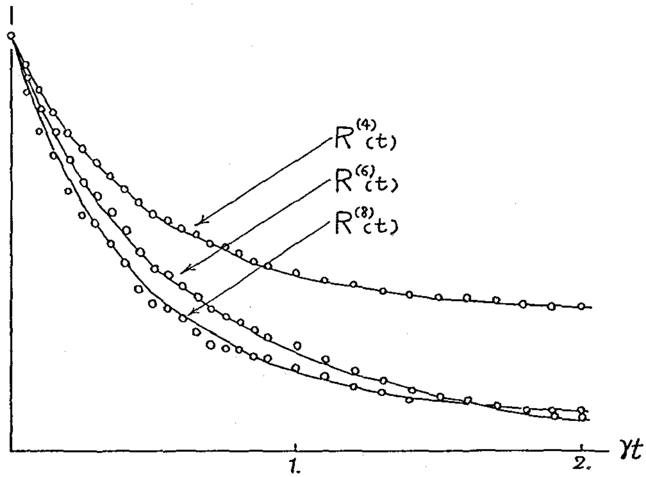

Fig. 8 - Higher order time correlation functions ($\mu = 100/\pi$).

correlation functions can be expanded into polynomials of the lowest order correlation function $R^{(2)}(t)$ as

$$R^{(4)}(t) \to 1 + 2R^{(2)}(t)^2$$

$$R^{(6)}(t) \to 3R^{(2)}(t)(3 + 2R^{(2)}(t)^2)$$

$$R^{(8)}(t) \to 3(3 + 24R^{(2)}(t)^2 + 8R^{(2)}(t)^4) \quad \text{etc.}$$

We examine whether the polynomial expansion is valid in our case; the results of polynomial expansion are indicated by circles in Fig.8, which fit very well with the solid curves. We may, therefore, conclude that the fully developed chaos obeys a Gaussian stochastic process.

The origin of the Gaussion behavior can be explained in the following way: From Eq.(2.2) $\phi(t)$ is expressed as

$$\phi(t) = \gamma\int_{-\infty}^{t} e^{-\gamma(t-s)} g(s)ds + \text{const} \quad ,$$

with

$$g(t) = 2B\pi\mu \cos(\phi(t - t_R) - \phi_0) \quad .$$

In the limit of large μ, the fluctuation of ϕ is much enhanced, and it takes a very small time (say τ_c) for ϕ to change by $O(\pi)$. The "delayed force" $g(t)$, therefore, changes its sign in a time scale of $O(\tau_c)$, and the correlation time of $g(t)$ is estimated to be $O(\tau_c)$. Since $\phi(t)$ is a linear superposition of such short lived forces $g(t)$, the motion of ϕ becomes a Gaussian one due to the central limit theorem.

The above explanation shows that within the time scale $O(\tau_c)$ the motion of $\phi(t)$ will significantly deviate from the Gaussian process. To show this we introduce the time flatness factor defined by

$$Q^{(2n)}(t) \equiv \langle(\phi(t) - \phi(0))^{2n}\rangle \,/\, \langle(\phi(t) - \phi(0))^2\rangle^n \quad ,$$

which is convenient in studying the statistics of a slight change of ϕ, and in the Gaussian process it reduces to a constant $(2n+1)!!$. We show in Fig.9 two time flatness factors $Q^{(4)}(t)$ and $Q^{(6)}(t)$ as functions of time. In a sufficiently short

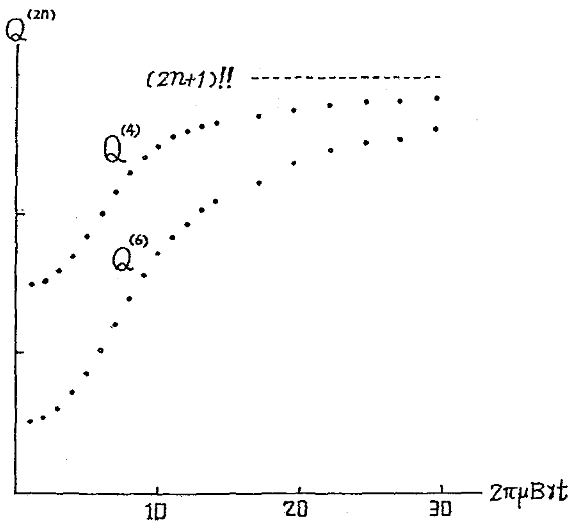

Fig.9 - Time flatness factors ($\mu = 100/\pi$).

time regime in the unit of $(2\pi\mu B\gamma)^{-1}$, they deviate significantly from the Gaussian value. They approach the Gaussian value for time greater then $20/(2\pi\mu B\gamma)$, which can be identified with the correlation time τ_c. The motion of ϕ looks gaussian on a coarse time scale larger than $20/(2\pi\mu B\gamma)$.

One can introduce an integrable stochastic model reproducing exactly the statistical properties of the shorter time behavior /8/. This problem is, however, a little complicated, and we do not go further into it in this article . Before closing this section, we summarize the bifurcation sequences leading to the fully developed chaos:

stationary state → square wave → successive period doubling bifurcations → square wave chaos → successive higher-harmonic bifurcations → developed chaos — ····· → fully developed chaos

The way of transitions from the developed chaos to the fully developed one looks so complicated that it is still not clear.

IV - OTHER KINDS OF INSTABILITIES

Nutation chaos - The delay induced instability takes place under the two conditions (1) $t_R\gamma \gg 1$ and (2) $A^2B > 1$; the latter condition means that the nonlinear phase shift ϕ is much larger than unity. In the inverse limit regime namely $t_R\gamma \ll 1$ and $\phi \ll 1$, a new kind of instability may occur. In this case Eq.(2.1a,b) can be approximated by a differential equation:

$$\dot{\xi}(t) = a - b\xi(t) + i[\eta(t) - \eta_0]\xi(t) \, , \tag{4.1a}$$

$$\dot{\eta}(t) = - \eta(t) + |\xi(t)|^2 , \tag{4.1b}$$

where $\tau \equiv t\gamma$, and the field and medium variablesare scaled as $(\xi,\eta) = (E/\sqrt{\tau_R}, \eta/\tau_R)$ $(\tau_R \equiv \gamma t_R)$. The parameter a, b, and η_0, which are defined by $A/\tau_R^{3/2}$, $(1-B)/\tau_R$ and ϕ_0/τ_R, respectively, are assumed to be quantities of the order of unity. Note that Eq.(4.1a) has the same form as the optical Bloch equation, if Reξ and Imξ are regarded as the two components of the Bloch vector. The total phase shift $(\eta - \eta_0)$ plays the role of the Rabi nutation frequency and b the damping one.

A characteristic of our system is that the Rabi nutation is self-induced as a result of interplay between ξ and η , if the cavity life time $t_R/(1-B)$ is longer than the medium relaxation time γ^{-1}, i.e. $b < 1$ /9/. The fundamental frequency of nutation is $a^{2/3}b^{-1/3}$, which is much longer than π/t_R, the frequency of the delay induced instability. This nutation becomes chaotic in a parameter domain where the three stationary solutions ("bistable" solution) exist. The negative slope solution acts as a saddle like fixed point, and it disturbs the regular nutation to a chaotic oscillation /9/.

Transversal chaos - The intensity distribution of the incident laser beam is not always homogeneous in its transversal direction. The nutation frequency $\omega_N = a^{2/3}b^{-1/3}$ is then inhomogeneous, and the cavity field tends to oscillate with different frequencies at different parts in the transversal direction. Usually, the diffraction is strong enough to entrain all the oscillations to a single frequency one. However if the laser beam has a strong transversal inhomogeneity overwhelming the diffractive coupling, one can expect that the mutual entrainment is destroyed and a transition to chaos occurs. The possibility of this type of chaos is being investigated by Davis and Ikeda.

The effect of the transversal inhomogeneity on the delay induced instability was investigated by Moloney et al /14/. They reported bifurcations through quasi-periodic oscillations and frequency locked ones, analogous to observed instabilities in fluid systems.

ACKNOWLEDGEMENTS -

The work reviewed here has been developed in cooperation with Professor O. Akimoto, Dr. H. Daido, Mr. K. Kondo and Mr. P. Davis. Friendly support by them is gratefully acknowledged. The author thanks Professor H. Hasegawa for his encouraging interest in this work.

REFERENCES

[1] Ruelle, D. and Takens, F., Commun. Math. Phys. 20 (1971) 167.
[2] Landau, L.D., and Lifshitz, E.M., Fluid Mechanics (Pergamon Press, London, (1959).
[3] Feigenbaum, M.J., J. Stat. Phys. 25 (1978) 25.
[4] Swinney, H.L. and Gollub, J.P., Phys. Today 41 (1978) August.
[5] For example, see Optical Bistability, edited by Bowden, C.M., Ciftan, M. and Robl, H.R. (Plenum Press, New York 1981).
[6] Ikeda, K., Opt commun. 30 (1979) 257; Ikeda, K., Daido, H., and Akimoto, O., Phys. Rev. Lett. 45 (1980) 709; Ikeda, K., Daido, H., and Akimoto, O., to be published.
[7] Ikeda, K. Kondo, K. and Akimoto, O., to be published.
[8] Ikeda, K. and Akimoto, O., to be published.
[9] Ikeda, K. and Akimoto, O., Phys. Rev. Lett. 48 (1982) 617.

[10] Firth, W.J., Opt. Commun. 39 (1981) 343; Abraham, E., Firth, W.J., and Carr,J., Phys. Lett. 69A (1982) 47.
[11] Winful, H.J. and Cooperman, G.D., Appl. Phys. Lett. 40 (1982) 298.
[12] Silberberg, Y. and Bar Joseph, I., Phys. Rev. Lett. 48 (1982) 1514.
[13] Carmichael, H.J., Savage, C.M., and Walls, D.F., to be published.
[14] Moloney, J.V., Hopf, F.A., and Gibbs, H.M., Phys. Rev. A25 (1982) 3442.
[15] Gibbs, H.M., Hopf, F.A., Kaplan, D.L., and Shoemaker, R.L., Phys. Rev. Lett. 46 (1981) 474; Hopf, F.A., Kaplan, D.L., Gibbs, H.M., and Shoemaker, R.L., Phys. Rev. A25 (1982) 2172.
[16] Nakatsuka, H., Asaka, S. Ito, H., and Matsuoka, M., to be published.